

THE OUTPUT CHARACTERISTIC OF A PHOTOVOLTAIC ARRAY UNDER MISMATCHING CONDITIONS

ĐẶC TÍNH ĐIỆN ĐẦU RA CỦA MỘT DÀN PIN MẶT TRỜI DƯỚI CÁC ĐIỀU KIỆN KHÔNG ĐỒNG NHẤT

Nguyen Duc Tuyen^{1,*}, Le Viet Thinh¹, Nguyen Quang Thuan²

ABSTRACT

In operating a photovoltaic (PV) system, the mismatching phenomenon is the most commonly occurring scenario among the PV modules of the PV arrays, causing the PV cells to operate under different conditions, which leads to significant power losses in the PV arrays. Prediction of the electrical performance of a PV array under mismatching conditions can improve the operational efficiency of a PV system. This paper proposes a simple and accurate method to extract the output characteristic of a PV array under mismatching conditions. The current-voltage (I-V) characteristic of a PV cell is represented by evaluating the single-diode model (SDM). After that, the I-V characteristic of a PV module and a PV array are simulated on the basis of the SDM. The effectiveness of the method is verified by an investigation conducted on a polycrystalline PV panel. The investigated results prove the proposed method is highly effective in simulating the I-V characteristic of a PV array under mismatching conditions.

Keywords: Photovoltaic; mismatching conditions; I-V characteristic; single-diode model; partial shading conditions.

TÓM TẮT

Trong vận hành hệ thống điện mặt trời, hiện tượng không đồng nhất thường xuyên xảy ra đối với các tấm pin mặt trời (PMT) trong một dàn PMT, làm cho các tế bào PMT hoạt động dưới các điều kiện rất khác nhau, từ đó công suất của dàn PMT bị tổn hao rất lớn. Việc dự đoán được đặc tính điện của một dàn PMT dưới các điều kiện không đồng nhất giúp nâng cao hiệu suất của hệ thống điện mặt trời. Bài báo này đề xuất một phương pháp đơn giản và chính xác để tìm ra được đặc tính điện đầu ra của một dàn PMT dưới các điều kiện không đồng nhất. Đặc tính dòng điện - điện áp của một tế bào PMT được trình bày dưới cả điều kiện lý tưởng và điều kiện không đồng nhất. Sau đó, đặc tính dòng điện - điện áp của tấm PMT và dàn PMT được phát triển trên cơ sở của đặc tính điện tế bào PMT. Tính hiệu quả của phương pháp được kiểm chứng trên một tấm PMT loại polycrystalline. Kết quả nghiên cứu cho thấy phương pháp được đề xuất có độ chính xác cao trong việc mô phỏng đặc tính dòng điện - điện áp của dàn PMT dưới các điều kiện không đồng nhất.

Từ khóa: Pin mặt trời; các điều kiện không đồng nhất; đặc tính dòng điện - điện áp; Mô hình một diode; các điều kiện che khuất.

¹Hanoi University of Science and Technology

²Hanoi University of Industry

*Email: tuyen.nguyenduc@hust.edu.vn

Received: 10/01/2020

Revised: 15/6/2020

Accepted: 25/4/2021

NOMENCLATURE

Symbol	Unit	Mean
a	-	Diode ideality factor
I	A	Current generated by the photovoltaic (PV) panel
I_d	A	Shockley diode current
I_{mpp}	A	Current at the maximum power point (MPP)
I_{pv}	A	Photovoltaic current
$I_{pv(G,T)}$	A	Photovoltaic current at other irradiance - temperature (T-G) conditions
I_{sat}	A	Reverse saturation current
$I_{sat(G,T)}$	A	Reverse saturation current at other T-G conditions
I_{sc}	A	Short-circuit current
K	J/K	Boltzmann constant (1.381×10^{-23} J/K)
K_i	A/°C	Thermal coefficient of the short-circuit current
K_v	V/°C	Thermal coefficient of the open-circuit voltage
N_s	-	Number of series-connected cells
q	C	Electron charge ($1.60217646 \times 10^{-19}$ C)
R_{sh}	Ω	Shunt resistance
R_s	Ω	Series resistance
V	V	Voltage generated by the PV panel
V_{mpp}	V	Voltage at the MPP
V_{oc}	V	Open-circuit voltage
T	K	Cell temperature
T_{ref}	K	Cell temperature at the Standard Test Condition (STC): 298.15 [K]
G	W/m ²	Irradiance
G_{ref}	W/m ²	Irradiance at the STC: 1000 W/m ²

ABBREVIATIONS

PV	Photovoltaic
PSCs	Partial shading conditions

I-V	Current versus Voltage
P-V	Power versus Voltage
MPP	Maximum power point
MPPT	Maximum power point tracking
GMPP	Global maximum power point
LMPP	Local maximum power point
SS	Simple series
SP	Series parallel
BL	Bridge-linked
HC	Honey comb
TCT	Total-cross-tied
SDM	Single-diode model

1. INTRODUCTION

The fast-paced growth of photovoltaic (PV) system has brought a lot of opportunities to develop sustainable energy in the world, but it also comes up with plenty of challenging problems baffling both operators and researchers. Indeed, operation a PV system, in reality, has to deal with many obstacles, including which come from the uncertainty of meteorology [1]. Non-uniform illumination becomes one of the most aspects can cause detrimental influences to PV arrays [2, 3].

For building-integrated PV and solar power plants in small spaces, the cells might be shaded by neighbouring cells [4]. These cases are referred as static shadows. Meanwhile, the dynamic shadows are phenomena such as the moving clouds, snow, bird dropping, leaves, etc.[5 [5, 6]. Operating a PV plant under partial shading conditions (PSCs) causes power losses of the system. In addition, the cells in the shaded areas cause hotspots in PV arrays, therefore the PV arrays can be damaged [4].

To mitigate these phenomena, a bypass diode is connected in parallel with a PV cell block to transfer the current through the shaded areas [3]. But this solution causes the power-voltage (P-V) characteristics of PV arrays have multiple maximum power points (MPPs), which is considered difficult for maximum power point tracking (MPPT) algorithm to track the global maximum power point (GMPP) [3].

To overcome this problem, this paper is dedicated to simulating the output characteristics of PV arrays under shading patterns to obtaining the GMPP. Simulations are run on four common PV configurations, which are series-parallel (SP), bridge-linked (BL), honeycomb (HC), and total-cross-tied (TCT). Since the single-diode model (SDM) has proved its advantages on identifying I-V and P-V characteristics of PV cells, it is developed to simulate the I-V and P-V characteristics of PV arrays.

2. ELECTRICAL MODEL OF A PV CELL AND PV MODULE

In order to evaluate effectively the behaviour of a PV cell, it is needed to adapt a model representing the

electrical characteristics of a PV cell. Figure 1 displays the equivalent circuit of the SDM, which is frequently utilized in the field study of PV [7, 8].

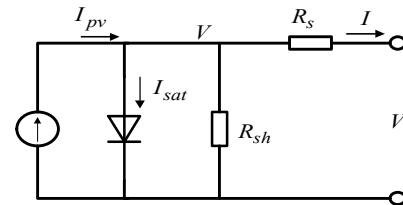


Figure 1. Equivalent circuit of the single-diode model

The behaviour of the solar cell is expressed by Equation (1):

$$I = I_{pv} - I_d - \frac{V + IR_s}{R_{sh}} = I_{pv} - I_{sat} \left(e^{\frac{V}{aV_t}} - 1 \right) - \frac{V + IR_s}{R_{sh}} \tag{1}$$

Where V_t is the thermal voltage defined by the following equation.

$$V_t = \frac{kT}{q} \tag{2}$$

Five parameters of the SDM, I_{pv} , I_{sc} , a , R_s , and R_{sh} are obtained from the manufactured datasheet, including the values of significant points of the I-V curve, $(I_{sc}, 0)$, $(0, V_{oc})$ and (I_{mpp}, V_{mpp}) . Solving Equation (1) is the key to obtain the I-V characteristic of a PV cell. Herein this task is conducted in a more general context, that is in a PV module as represented as follows.

2.1. The I-V and P-V characteristics of a PV module under uniform condition

PV generators are made of a number of PV cells connected in series and in parallel, not referred to a single PV cell. The operating voltage of the PV cell is few hundreds of millivolts, while the current generated at high irradiation levels is of some amperes. As a result, to reach the desired voltage, a number of connected-series cells are arranged into PV modules. So some approaches, [9] and [10], have used a modified expression of Equation (1) as follow:

$$I = I_{pv} - I_{sat} \left(e^{\frac{V}{aN_s V_t}} - 1 \right) - \frac{V + IR_s}{R_{sh}} \tag{3}$$

Applying Equation (3) under three remarkable points, such that the short-circuit point, the open-circuit point, the maximum power point (MPP), produces the following equations:

- At short-circuit point ($I = I_{sc}$, $V = 0$):

$$I_{sc} = I_{pv} - I_{sat} \left[\exp \left(\frac{R_s I_{sc}}{aN_s V_t} \right) - 1 \right] - \frac{I_{sc} R_s}{R_{sh}} \tag{4}$$

- At open-circuit point ($I = 0$, $V = V_{oc}$):

$$0 = I_{pv} - I_{sat} \left[\exp \left(\frac{V_{oc}}{aN_s V_t} \right) - 1 \right] - \frac{V_{oc}}{R_{sh}} \tag{5}$$

• At the MPP ($I = I_{mpp}$, $V = V_{mpp}$):

$$I_{mpp} = I_{pv} - I_{sat} \left[\exp\left(\frac{V_{mpp} + R_s I_{mpp}}{a N_s V_t}\right) - 1 \right] - \frac{V_{mpp} + R_s I_{mpp}}{R_{sh}} \quad (6)$$

Since these equations contain the exponential functions and five variables, it can not be solved straight away. To deal with this problem, an iterative method is proposed as follow. The second term in (3) is assumed can be neglected [8], the photovoltaic current is rewritten as in Equation (7).

$$I_{pv} = I_{sc} \frac{R_s + R_{sh}}{R_{sh}} \quad (7)$$

The parallel resistance is calculated by substituting Equation (7) into Equation (6), as in Equation (8).

$$R_{sh} = \frac{I_{sc} R_s - V_{mpp} - I_{mpp} R_s}{I_{mpp} + I_{sat} \left[\exp\left(\frac{V_{mpp} + I_{mpp} R_s}{a N_s V_t}\right) - 1 \right] - I_{sc}} \quad (8)$$

By assuming the denominator of the right side of Equation (8) is zero, the maximum value of the series resistance is calculated as in Equation (9).

$$R_{s,max} = \frac{a N_s V_t \ln\left(\frac{I_{sc} - I_{mpp}}{I_{sat}} - 1\right) - V_{mpp}}{I_{mpp}} \quad (9)$$

After that, the photovoltaic current, the reverse saturation current and the diode's ideality factor are calculated by equations (4)-(6), respectively. This process continues with the value of the series resistance ranging from $[0, R_{s,max}]$.

For two points in the P-V curve of a PV panel, one is on the left side and another is on the right side, the value of the slope of the P-V curve respect to the point at the left side is greater than zero and for the point at the right side would be smaller than zero.

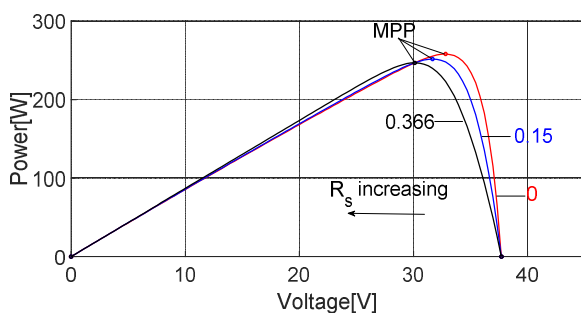


Figure 2. P-V curves with different values of R_s

As can be seen in Figure 2, when the series resistance increases, the peak of the P-V curve will shift from the right side of this fixed point to the left side. Consequently, the derivative of the power with respect to the voltage will monotonically decrease from the positive to negative.

As a result, the process stops until the condition (10) is satisfied.

$$\left(\frac{dP}{dV}\right)_i \left(\frac{dP}{dV}\right)_{i-1} < 0 \quad (10)$$

Using the interpolation method, the value R_s is calculated as Equation (11).

$$R_s = R_{s,i} + (R_{s,i} - R_{s,i-1}) \frac{\left(\frac{dP}{dV}\right)_{i-1}}{\left(\frac{dP}{dV}\right)_{i-1} - \left(\frac{dP}{dV}\right)_i} \quad (11)$$

Where i is the number of points, in which derivative of the power with respect to the voltage is greater than zero.

2.2. The I-V and P-V characteristics of a PV module under PSCs

In the previous section, the SDM is scaled up under the hypothesis that all the cells operate in the same condition. However, this situation is far further from what happens in real life since the PV array is greatly affected by external aspects. Nonuniform illumination causes the cells of a PV module operating in very different irradiance levels. By considering the effects of new T-G conditions on the operation of a PV cell, the photovoltaic current and saturation current are calculated as in Equation (12) and Equation (13), respectively.

$$I_{pv}(G, T) = \left[I_{pv} + K_i (T - T_{ref}) \right] \frac{G}{G_{ref}} \quad (12)$$

$$I_{sat}(G, T) = \frac{I_{sc} + K_i (T - T_{ref})}{e^{\frac{V_{oc} + K_v (T - T_{ref})}{a V_t}} - 1} \quad (13)$$

Where $I_{pv}(G, T)$, $I_{sat}(G, T)$ are the photovoltaic current and saturation current at other T-G conditions, respectively. K_i and K_v are the thermal coefficient of the short-circuit current and the open-circuit voltage, respectively. Three other parameters of PV cell (R_s , R_{sh} , a) are assumed to be unchanged at other T-G conditions. Consequently, the corresponding SDM for a shaded PV module is represented as in Figure 3.

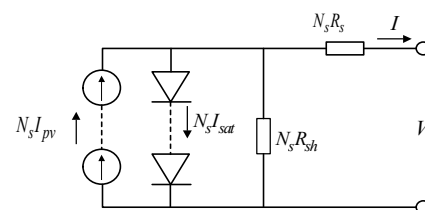


Figure 3. Equivalent circuit of PV module of N_s series-connected PV cells Equation (1) now becomes Equation (14).

$$I(G, T) = N_s I_{pv}(G, T) - N_s I_{sat}(G, T) \left(e^{\frac{V(G, T)}{a N_s V_t}} - 1 \right) - \frac{V(G, T) + I(G, T) N_s R_s}{N_s R_{sh}} \quad (14)$$

Where $I(G, T)$ and $V(G, T)$ are the output current and output voltage of the PV module, respectively. In Figure 4,

the polycrystalline Kyocera KC175 GHT-2 PV module composes of the first 16 PV cells operating at 1000W/m^2 , the 16 sequential PC cells operating at 600W/m^2 and the 16 final PV cells operating at 300W/m^2 . By connected three strings of 16-series-connected PV cells in Matlab/Simulink, the I-V and P-V characteristics of this PV module are demonstrated under uniform condition and PSCs as in Figure 5. The output characteristics have more than one MPP caused by the insertion of bypass diode, and the maximum output power also decreases.

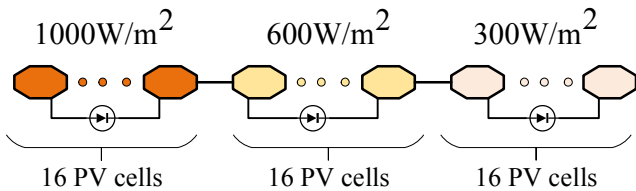


Figure 4. Model of a PV module with bypass diodes under partial shading conditions

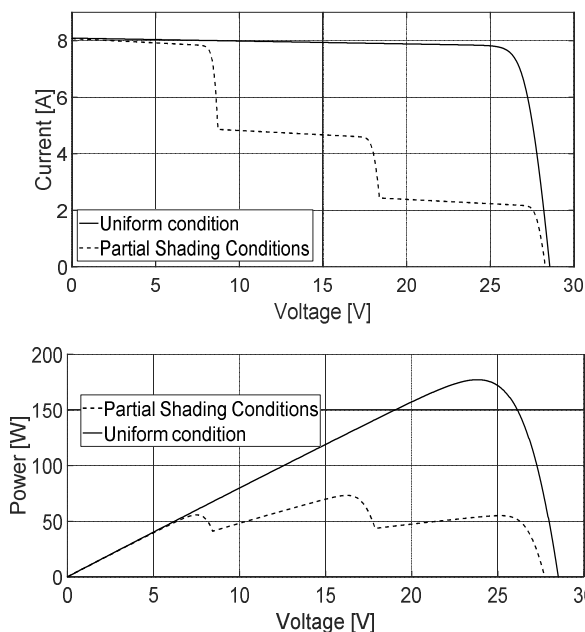


Figure 5. I-V and P-V characteristics of Kyocera KC175 GHT-2 PV module under the uniform condition and PSCs

3. PV ARRAY SIMULATION ON MATLAB/SIMULINK

3.1. Effects on the I-V and P-V characteristics of a PV array

When considering the effects of PSCs on a PV array, besides irradiance and temperature, the PV array configuration and shading pattern also have significant impacts on the I-V and P-V characteristics of a PV array. In practical situations, the shading pattern is random, so the only thing can be controlled to mitigate effects of PSCs is the PV array configuration. Analyzing the I-V characteristic of PV array for each PV array configuration is the key to choosing suitable PV array configuration. However, since Equation (1) is an implicit equation and each PV module operating under various T-G conditions will have different I-V characteristics. Therefore, to obtain the equivalent I-V

characteristic of a PV array under mismatching conditions, a Matlab/Simulink-based model is established. This PV array model composes a number of PV modules applied SDM. Four PV array model with different configurations, e.g., SP, BL, HC, and TCT, are used. The T-G values of these model are changeable.

The PV array configuration is the way of arranging the PV modules in a PV array to mitigate the partial shading losses. In [11], different PV array configurations are analyzed, including SS, SP, TCT, BL and HC, which are represented in Figure 6. Among these PV configurations, SP, BL, HC and TCT have been proved to be their superiorities on reducing the power losses caused by partial shading. Therefore, in this paper, these four array configurations are chosen to apply SDM in simulating the I-V and P-V characteristics of a PV array.

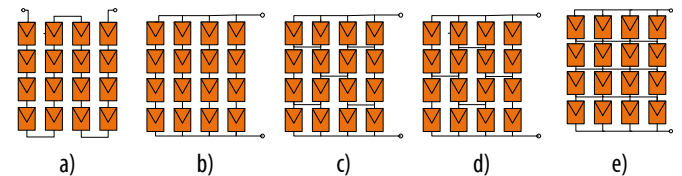


Figure 6. Five PV configurations: a) SS; b) SP; c) BL; d) HC; e) TCT

In addition, the shading pattern is important to evaluate the performance of a PV array under PSCs. Herein five shading topologies are considered with the shading area is $\frac{1}{4}$ the total area of PV array, including row shading, column shading, diagonal shading, block-shaped shading and random shading. These PV shading patterns are illustrated as in Figure 7.

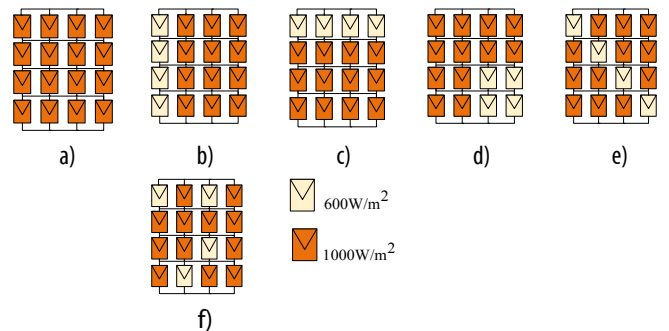


Figure 7. Shading patterns of a PV array: a) uniform; b) column shading; c) row shading; d) block-shaped shading; e) diagonal; f) random shading

3.2. Simulation results and discussions

Four PV array configurations, which are SP, BL, HC, and TCT, are simulated with six afore-mentioned PV patterns on the Kyocera KC175 GHT-2 PV array. The I-V and P-V characteristics of this PV array in all scenarios are plotted as in Figure 8.

As can be seen from Figure 8, in six scenarios, under the PSCs, the P-V curves have two local maximum power points, expect under the column shading and diagonal shading by BL and TCT configurations. The I-V curve under random shading varies a lot when changing the PV configuration. The output power of the PV array under row

shading is the most detrimental since its GMPP is lowest in all situations. The column shading is the most beneficial since it's I-V and P-V curves have one MPP and the output maximum powers are highest. The I-V and P-V curves of PV array by three configurations, that are BL, HC and TCT, have many similarities. This can be explained by the correlation between these PV configurations since the BL and HC can be considered as subsets of TCT configuration.

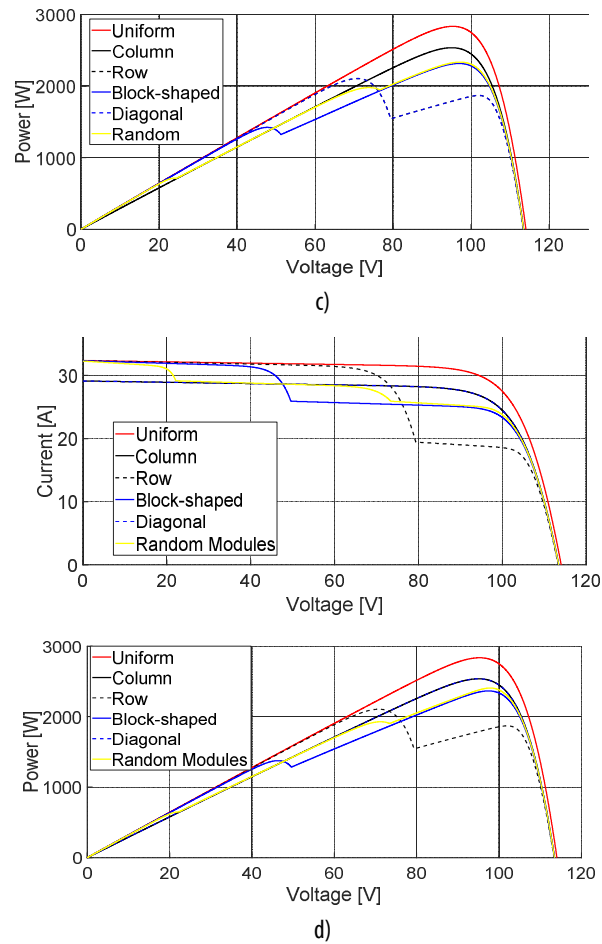
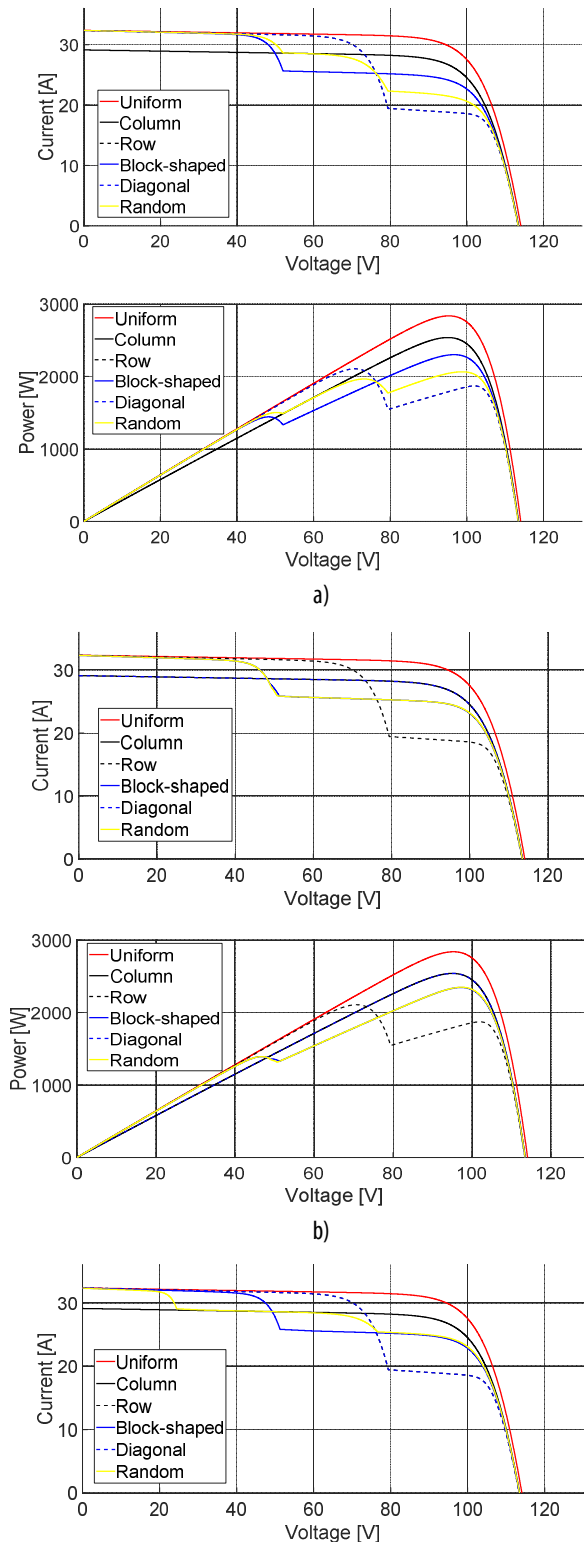


Figure 8. I-V and P-V characteristics of the Kyocera KC175 GHT-2 PV array by four configurations: a) SP; b) BL; c) HC; d) TCT

Figure 9 illustrates the power losses among five shading scenarios, which is calculated by Equation (15).

$$\Delta P_L = \frac{P_M - P_{MPS}}{P_M} \cdot 100 \tag{15}$$

The row shading causes the highest power losses in almost cases, above 25%. The block-shaped and random shadings are the second and third highest power losses, upper 15%. The least affected scenarios are the column shading with the power losses above 10%.

Shortly, the data in Figure 9 illustrate that at least above 10% of the output power of a PV array losses by the partial shading effect. This is a significant loss in operating a PV system. Demonstrating the I-V and P-V characteristic is the first step in detection the partial shading losses [4, 12]. The results of this research are vitally important in studying advanced MPPT algorithm to optimize the output power of a PV array [13-15]. This method can be used as an alternative method to track the GMPP of a PV array as it provides all the values of power-voltage for each T-G conditions. This approach is more straightforward than the conventional MPPT algorithms, Perturb and Observe and Incremental Conductance, as the conventional methods can be misleading to track the MPP of a PV array under PSCs [15].

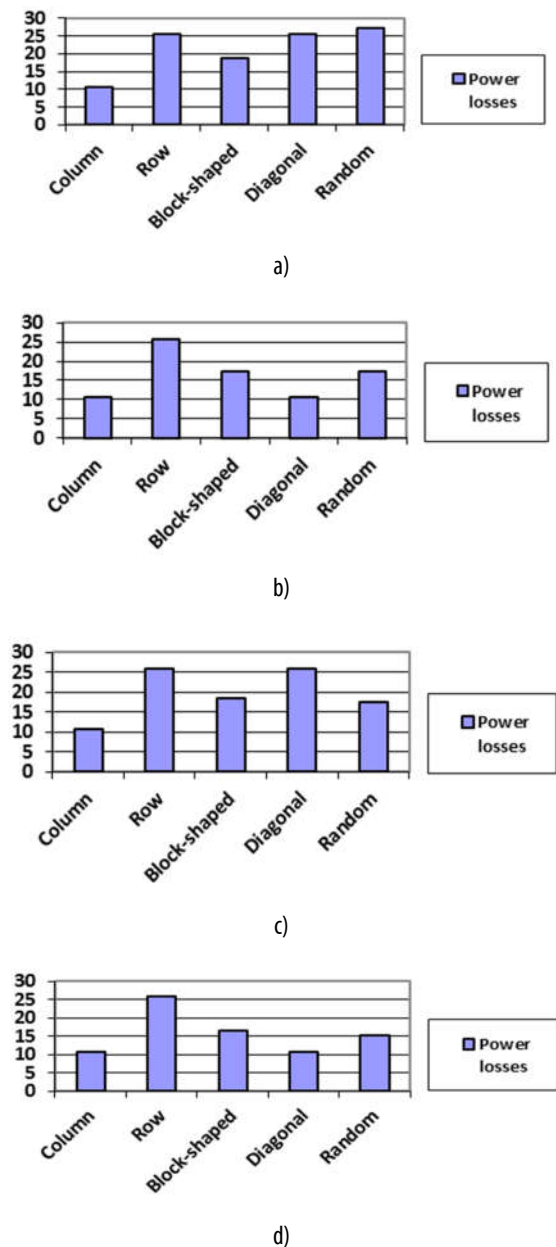


Figure 9. The power losses of PV array under five shading patterns: a. SP b. BL c. HC d. TCT

Since the partial shading closely relates to the fast-changing irradiance and temperature, obtaining I-V and P-V characteristics of a PV array in a specific period when changing both irradiance and temperature is an essential work in the future. When it comes to this work, forecasting the meteorology of the PV array location is needed, as well.

4. CONCLUSIONS

In this paper, the SDM is introduced to obtain the I-V and P-V characteristics of a PV module. By employing this model, the I-V and P-V characteristics of a PV array are simulated under both uniform and PSCs on Matlab/Simulink. The data shows the large impact of partial shading on a PV array since the power losses are at least above 10%. After analyzing five common shading patterns,

the column shading is considered the most beneficial scenario for a PV array under PSCs. Since the proposed model has proved its effectiveness, it can be applied to forecasting the output power of a PV array.

REFERENCES

- [1]. Ding K, Bian X, Liu H, Peng T, 2012. *A MATLAB-simulink-based PV module model and its application under conditions of nonuniform irradiance*. IEEE Trans. Energy Convers. 27, 864–72.
- [2]. Lyden S, Haque M E, 2019. *Modelling, parameter estimation and assessment of partial shading conditions of photovoltaic modules*. J. Mod. Power Syst. Clean Energy. 7, 55–64.
- [3]. Bai J, Cao Y, Hao Y, Zhang Z, Liu S, Cao F, 2015. *Characteristic output of PV systems under partial shading or mismatch conditions*. Sol. Energy. 112, 41–54.
- [4]. Nguyen D, Lehman B, 2008. *An adaptive solar photovoltaic array using model-based reconfiguration algorithm*. IEEE Trans. Ind. Electron. 55, 2644–54.
- [5]. Sai Krishna G, Moger T, 2019. *Reconfiguration strategies for reducing partial shading effects in photovoltaic arrays: State of the art*. Sol. Energy. 182, 429–52.
- [6]. Petrone G, Serra F, Spagnuolo G, Monmasson E, 2019. *SoC implementation of a photovoltaic reconfiguration algorithm by exploiting a HLS-based architecture*. Math. Comput. Simul. 158, 520–37.
- [7]. Celik A N, Acikgoz N, 2007. *Modelling and experimental verification of the operating current of mono-crystalline photovoltaic modules using four- and five-parameter models*. Appl. Energy. 84, 1–15.
- [8]. Cubas J, Pindado S, Victoria M, 2014. *On the analytical approach for modeling photovoltaic systems behavior*. J. Power Sources. 247, 467–74.
- [9]. Laudani A, Riganti Fulginei F, Salvini A, 2014. *Identification of the one-diode model for photovoltaic modules from datasheet values*. Sol. Energy. 108, 432–46.
- [10]. Hussein A, 2017. *A simple approach to extract the unknown parameters of PV modules*. Turkish J. Electr. Eng. Comput. Sci. 25, 4431–44.
- [11]. Pendem S R, Mikkili S, 2018. *Modelling and performance assessment of PV array topologies under partial shading conditions to mitigate the mismatching power losses*. Sol. Energy. 160, 303–21.
- [12]. Dhimish M, Badran G, 2020. *Current limiter circuit to avoid photovoltaic mismatch conditions including hot-spots and shading*. Renew. Energy. 145, 2201–16.
- [13]. Gosumbonggot J, Nguyen D D and Fujita G, 2018. *Partial Shading and Global Maximum Power Point Detections Enhancing MPPT for Photovoltaic Systems Operated in Shading Condition*. Proc.53rd Int, Univ, 2018. Power Eng. Conf. UPEC, 1–6.
- [14]. Eltamaly A M, Al-Saud M S, Abokhalil A G, Farh H M H, 2019. *Photovoltaic maximum power point tracking under dynamic partial shading changes by novel adaptive particle swarm optimization strategy*. Trans. Inst. Meas. Control, 1-12.
- [15]. Gosumbonggot J, Fujita G, 2019. *Partial shading detection and global maximum power point tracking algorithm for photovoltaic with the variation of irradiation and temperature*. Energies.12, 202.

THÔNG TIN TÁC GIẢ

Nguyễn Đức Tuyên¹, Lê Viết Thịnh¹, Nguyễn Quang Thuấn²

¹Trường Đại học Bách khoa Hà Nội

²Trường Đại học Công nghiệp Hà Nội